Expanded View Figures

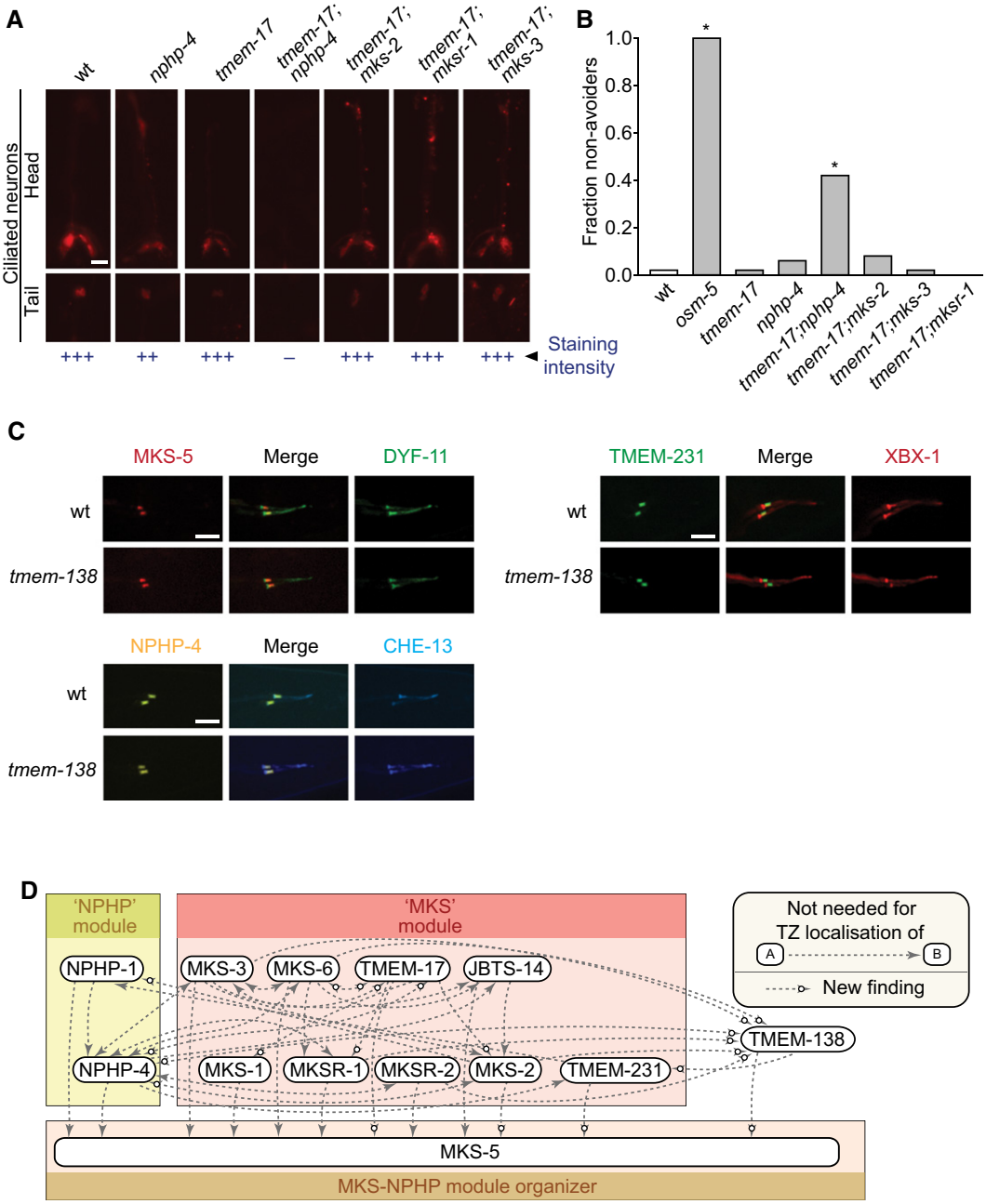

Figure EV1. *tmem-17* loss-of-function phenotypes, TZ markers in *tmem-138* mutants, and TZ negative interaction hierarchy data.

A Disruption of *tmem-17* alone does not cause overt ciliary defects as measured by uptake of fluorescent dye through environmentally exposed cilia. *tmem-17;nphp-4* double mutants are defective in dye uptake while *tmem-17;mks-2*, *tmem-17;mksr-1* and *tmem-17;mks-3* take up the dye similar to *tmem-17* alone. Scale bar: 20 μm.

B *tmem-17* mutants avoid high-osmolarity solutions, as do *tmem-17;mks-2*, *tmem-17;mksr-1*, and *tmem-17;mks-3* double mutants. *tmem-17;nphp-4* double mutants are partially defective in sensing osmolarity, though not as severely as *osm-5* (IFT mutant) animals, which are completely oblivious of the hyperosmotic barrier (*$P < 0.0001$, chi-squared test).

C TZ markers expressed in wild-type and the *tmem-138* mutants. MKS-5, TMEM-231 (MKS module), and NPHP-4 (NPHP module) do not require TMEM-138 for TZ localisation. Scale bars: 4 μm.

D Model showing all of the negative interaction amongst MKS/NPHP proteins, where a particular MKS/NPHP protein (at the arrowhead) is localised properly in a specific TZ mutant; a white circle on the arrowhead indicates new data obtained in this study.

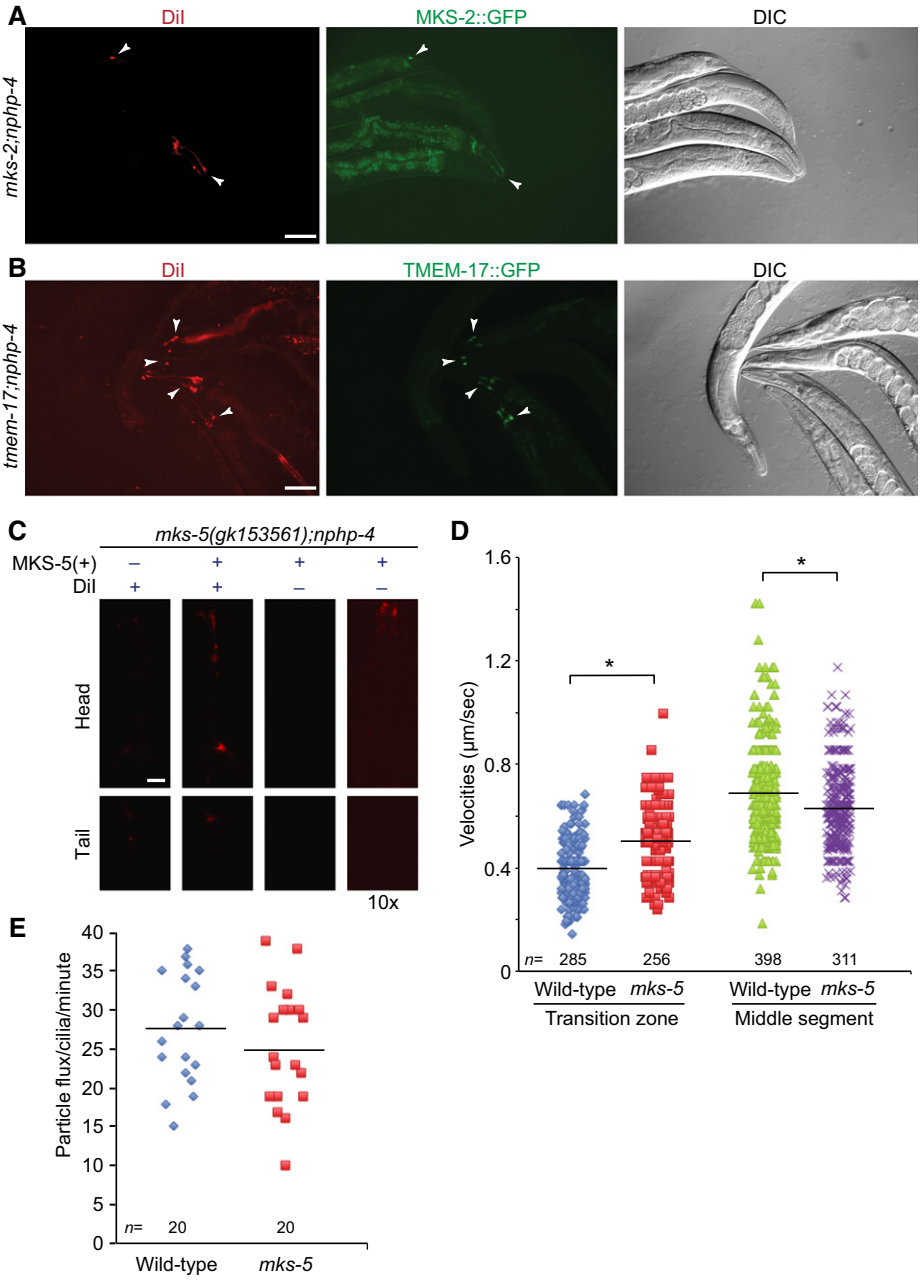

Figure EV2. Rescue of the dye-filling defective phenotype (Dyf) of *mks-2;nphp-4*, *tmem-17;nphp-4*, and *mks-5(gk153561);nphp-4* with the respective translational reporters, as well as IFT velocities and flux for wild-type and *mks-5* mutant animals.

A *mks-2;nphp-4* mutants display a failure to uptake the lipophilic dye DiI which can be rescued by the wild-type MKS-2::GFP reporter. Shown are transgenic animals (arrowheads) that express the reporter and uptake of the dye, while their nontransgenic siblings cannot uptake the dye. Scale bar: 100 µm.

B *tmem-17;nphp-4* mutants display a failure to uptake the lipophilic dye DiI which can be rescued by the wild-type TMEM-17::GFP translational reporter. Shown are transgenic animals (arrowheads) that express the reporter and uptake of the dye, while their nontransgenic siblings cannot uptake the dye. Scale bar: 100 µm.

C The *mks-5(gk153561);nphp-4* mutants display a Dyf phenotype, which can be rescued with expression of the wild-type MKS-5::tdTomato translational reporter. In the third set of head and tail panels, transgenic worms are shown at the same exposure time, but the signal is not detectable. In the right-hand set of panels, a tenfold longer exposure shows detectable signal for the MKS-5::tdTomato reporter, indicating that the signal for the transgenic worms is coming from the dye. Scale bar: 20 µm.

D Scatter plots of measured IFT velocities for wild-type and *mks-5* mutants using the CHE-13::YFP translational reporter. In the transition zone (TZ; proximal ~0.8 µm of the cilium), the mean IFT velocity is 0.39 µm/s in wild-type animals, but increases to 0.49 µm/s in the *mks-5* mutant, which lacks a detectable TZ. In the middle segment, mean IFT velocity is 0.69 µm/s, while in the *mks-5* mutant, it is significantly slower at 0.63 µm/s. *$P < 0.001$, *t*-test.

E IFT flux (in particles per minute) is shown for wild-type and *mks-5* mutants. No difference is observed between the flux of IFT particles in wild-type and *mks-5* animals ($P > 0.05$, *t*-test).

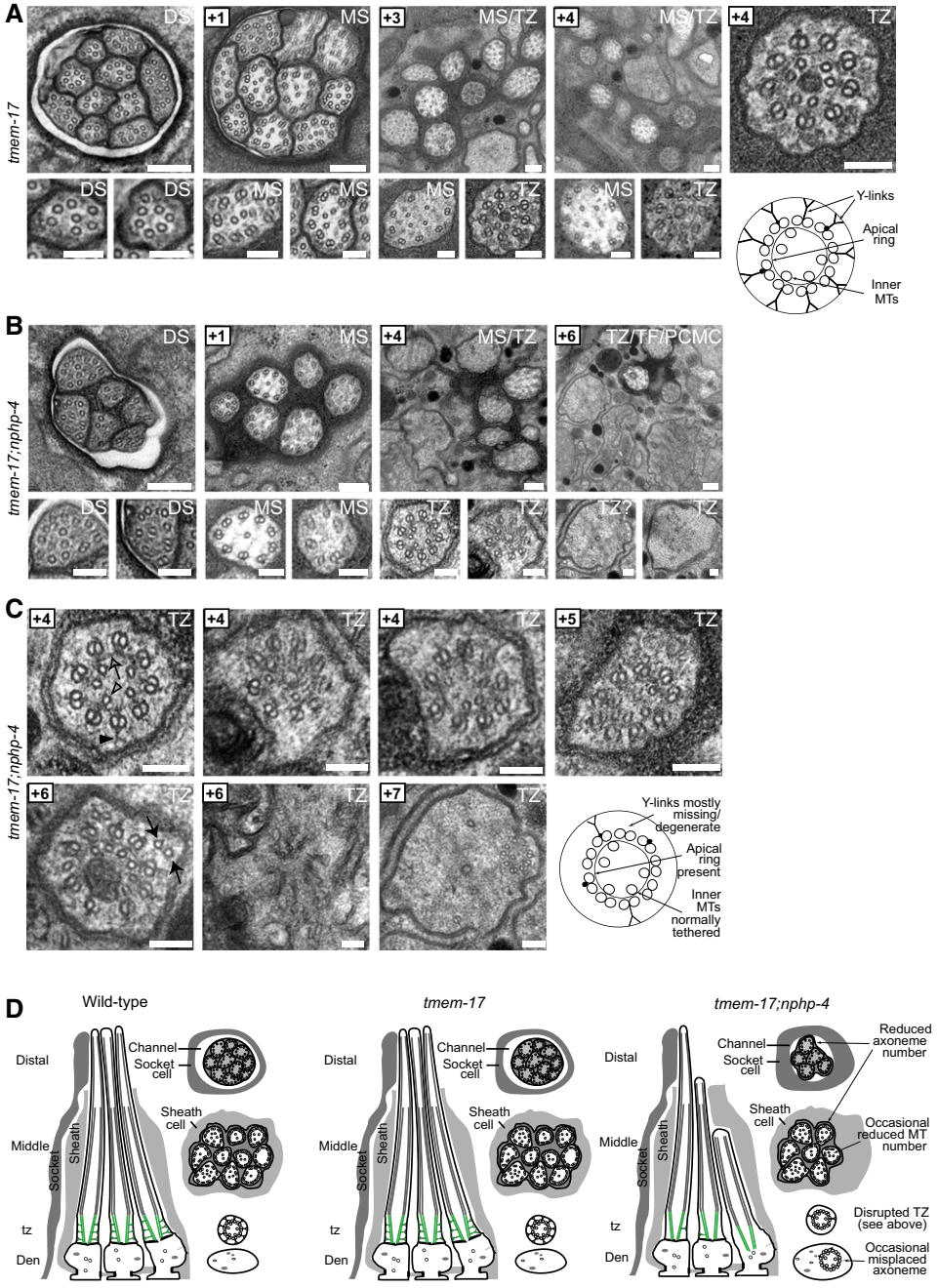

Figure EV3. Transmission electron microscopy of *tmem-17* and *tmem-17;nphp-4*.

Shown are serial cross-section images of amphid channel cilia at high and low magnification (mag.). For each set of images, boxed numbers denote proximal positioning of section relative to left-most (anterior) sections.

A *tmem-17* mutant cilium ultrastructure is similar to wild-type worms, possessing all characteristic features, including singlet microtubules (MTs) in the distal segments (DSs), an ordered ring of doublet MTs surrounding internal singlet MTs in the middle segments (MSs), and transition zones (TZ) possessing Y-links and an apical ring tethering inner singlet MTs to outer doublet MTs. Scale bars: 200 nm (low-mag. images); 100 nm (high-mag. images).

B, C In *tmem-17;nphp-4* double mutants, 3–4 middle and distal segments are missing and remaining axonemes sometimes possess missing doublet MTs. Most TZs lack some Y-link structure (closed arrowhead), and frequently other defects are observed, such as ectopic singlet MTs (closed arrow), reduced MT numbers (+7 image), and detachment from the ciliary/dendritic membrane (+7 image) indicative of an axoneme misplaced within the dendrite (see schematic). The apical membrane (open arrow) tethering inner singlet MTs (open arrowhead) to outer doublet MTs remains largely intact. Together, these ultrastructural defects are characteristic of mutants that carry a mutation in a member of both the NPHP module (*nphp*-4) and the MKS module (*tmem-17*). Scale bars: 200 nm (low-mag. images in B); 100 nm (high-mag. images in B and in C).

D Schematics summarising the ultrastructure phenotypes.

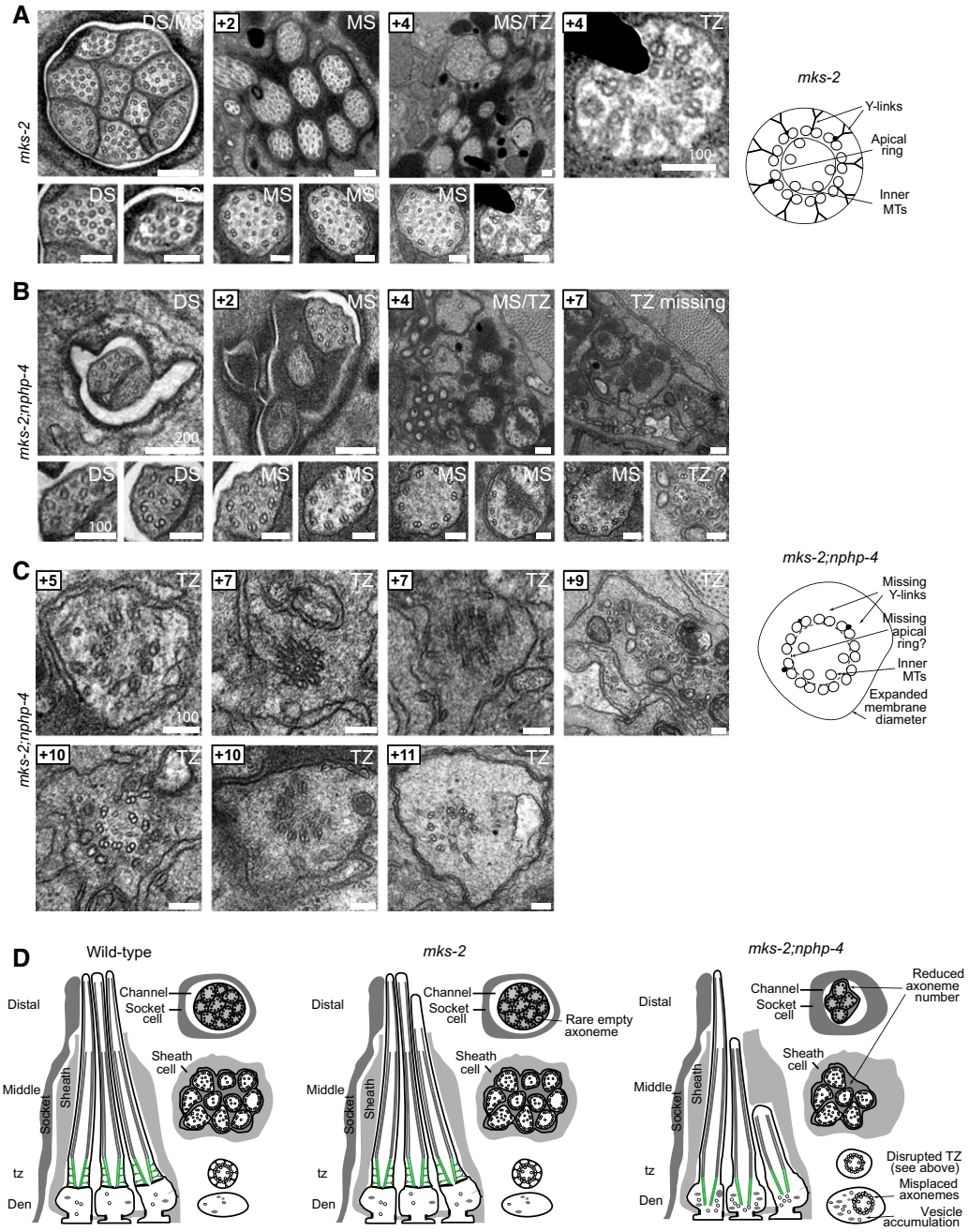

Figure EV4. Transmission electron microscopy of *mks-2* and *mks-2;nphp-4*.

Shown are serial cross-section images of amphid channel cilia at high and low magnification (mag.). For each set of images, boxed numbers denote proximal positioning of section relative to left-most section.

A *mks-2* mutant cilium ultrastructure is mostly similar to wild-type worms, possessing all characteristic features, including singlet microtubules (MTs) in the distal segments (DSs), an ordered ring of doublet MTs surrounding internal singlet MTs in the middle segments (MSs), and transition zones (TZ) possessing Y-links and an apical ring tethering inner singlet MTs to outer doublet MTs. However, occasional axonemes possess abnormal numbers of singlet or doublet MTs (bottom-left image). Scale bar: 200 nm (low-mag. images); 100 nm (high-mag. images).

B, C In *mks-2;nphp-4* double mutants, many middle and distal segments are missing. TZs completely lack Y-links and are detached from the ciliary/dendritic membrane indicative of axonemes anchored within the dendrite (i.e. misplaced; see schematic). The apical membrane that tethers inner singlet MTs to outer doublet MTs is difficult to discern, and doublet MTs are frequently disorganised (+10 image; left). Misplaced TZs are often surrounded by abnormal membrane (vesicle-like) accumulations (+5, +9, +10 images). These ultrastructural defects are characteristic of mutants that carry a mutation in both a member of the NPHP module (*nphp-4*) and the MKS module (*mks-2*). Scale bars: 200 nm (low-mag. images in B); 100 nm (high-mag. images in B and in C).

D Schematics summarising the ultrastructure phenotypes.

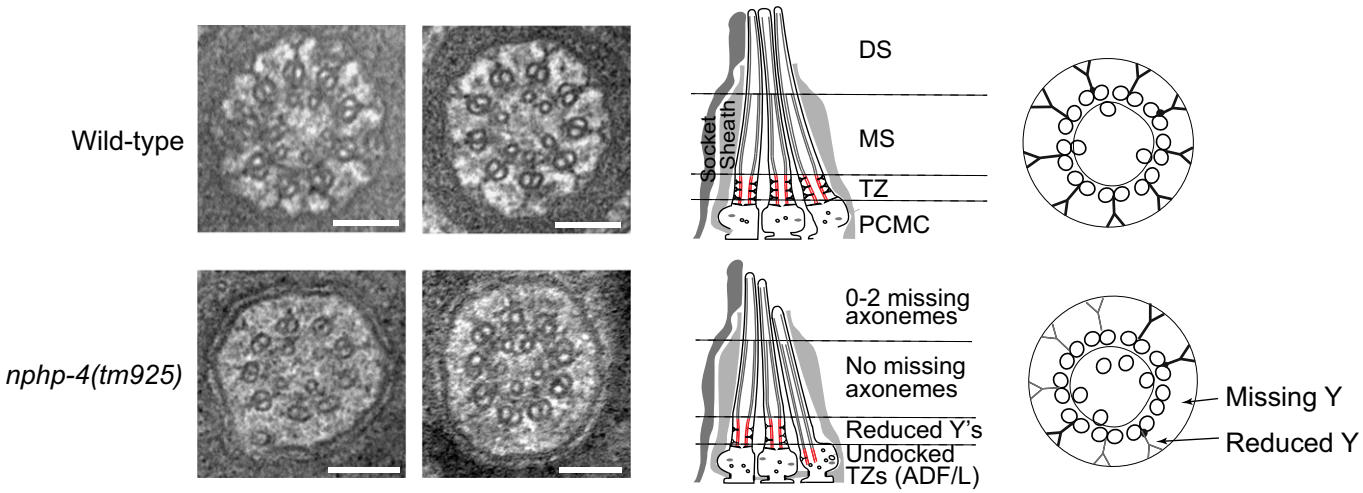

Figure EV5. Transmission electron microscopy of *nphp-4*.
Shown are cross-section images of amphid channel cilia at the transition zone. In *nphp-4* mutants, transition zone Y-links are often missing and when present have lower electron density (light grey) compared to wild type. Schematics on the right summarise the ultrastructure phenotypes. Scale bars: 100 nm.